Formation of Impact Craters

The processes by which large impact craters form, and the sudden releases of huge quantities of energy involved, cannot be duplicated in the laboratory, and, fortunately, no such structure has formed during recorded human history. All our knowledge about large impact structures is therefore indirect, and it has come from combining several areas of once-separate research: theoretical and experimental studies of shock waves (for reviews and literature, see *Melosh,* 1989), experimental production of small craters (e.g., *Gault et al.,* 1968; *Gault,* 1973; *Holsapple and Schmidt,* 1982, 1987; papers in *Roddy et al.,* 1977), and geological studies of larger terrestrial impact structures (*Shoemaker,* 1963; *Dence,* 1968; *Dence et al.,* 1977; *Grieve and Cintala,* 1981; *Grieve et al.,* 1981; *Schultz and Merrill,* 1981; *Stöffler et al.,* 1988). The cratering process is complex, many details are still uncertain, and neither calculations nor predictions can be made with firm confidence. But these studies provide the essential basis for understanding how impact craters form and for deciphering the geological features they display.

3.1. SHOCK WAVES AND CRATER FORMATION

The general term "impact crater" is used here to designate a **hypervelocity impact crater**, the structure formed by a cosmic projectile that is large enough and coherent enough to penetrate Earth's atmosphere with little or no deceleration and to strike the ground at virtually its original cosmic velocity (>11 km/s). Such projectiles tend to be relatively large, perhaps >50 m in diameter for a stony object and >20 m for a more coherent iron one.

Smaller projectiles, typically a few meters or less in size, behave differently in passing through the atmosphere. They lose most or all of their original velocity and kinetic energy in the atmosphere through disintegration and ablation, and they strike the ground at speeds of no more than a few hundred meters per second. In such a low-velocity impact, the projectile penetrates only a short distance into the target (depending on its velocity and the nature of the target material), and the projectile's momentum excavates a pit that is slightly larger than the projectile itself. The projectile survives, more or less intact, and much of it is found in the bottom of the pit. Such pits, sometimes called **penetration craters** or **penetration funnels**, are typically less than a few tens of meters in diameter.

Examples of these features include Brenham (Kansas), the many small pits made by the Sikhote-Alin (Russia) meteorite shower in 1947, and the pit dug by the largest piece of the Kirin (China) meteorite fall in 1976. The process of excavation is strictly a mechanical one, and high-pressure shock waves are not produced.

In sharp contrast, a **hypervelocity impact crater** starts to form at the instant that an extraterrestrial object strikes the ground surface at its original cosmic velocity. These impact velocities are much greater than the speed of sound in the target rocks, and the crater is produced by intense **shock waves** that are generated at the point of impact and radiate outward through the target rocks. Shock waves are intense, transient, high-pressure stress waves that are not produced by ordinary geological processes (for details, see *Melosh,* 1989, Chapter 3 and references therein). Peak shock pressures produced at typical cosmic encounter velocities may reach several hundred GPa. These pressure are far above the stress levels (~1 GPa) at which terrestrial rocks undergo normal elastic and plastic deformation, and the shock waves produce unique and permanent deformation effects in the rocks through which they pass.

The shock waves radiate from the impact point at high velocities that may exceed 10 km/s, much greater than the speed of sound in the target rocks. As they expand, they interact with the original ground surface to set a large volume of the target rock into motion, thus excavating the impact crater. The formation of an impact crater by shock waves,

and the immediate modification of the newly formed crater by gravity and rock mechanics, is a complex and continuous process. However, it is convenient to divide this process, somewhat arbitrarily, into three distinct stages, each dominated by different forces and mechanisms: **contact and compression**, **excavation**, and **modification** (*Gault et al.,* 1968; see also *Melosh,* 1989, Chapters 4, 5, and 8).

3.1.1. Contact/Compression Stage

This stage begins at the instant that the leading edge of the moving projectile makes contact with the ground surface. If the target is solid rock, the projectile is stopped in a fraction of a second and penetrates no more than 1–2× its own diameter (Fig. 3.1) before its immense kinetic energy is transferred to the target rocks by shock waves generated at the interface between projectile and target (*Kieffer and Simonds,* 1980; *O'Keefe and Ahrens,* 1982, 1993; *Melosh,* 1989, Chapter 4).

The general features of this conversion of kinetic energy into shock waves have been determined from experiments and theoretical studies (e.g., *O'Keefe and Ahrens,* 1975, 1977, 1993; *Ahrens and O'Keefe,* 1977; papers in *Roddy et al.,* 1977; *Melosh,* 1989, Chapter 4), although many details are still not well understood. One clear result is that, as one set of shock waves is transmitted outward from the interface into the target rocks, a complementary shock wave is reflected back into the projectile (Fig. 3.1) (*Melosh,* 1989, Chapter 4; *O'Keefe and Ahrens,* 1993).

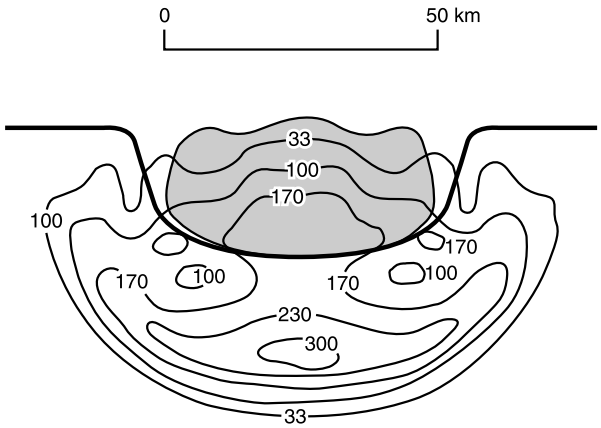

Fig. 3.1. Contact/compression stage: shock-wave generation and projectile deformation. Theoretical cross-section showing calculated conditions immediately after the impact of a large, originally spherical, projectile (stippled) onto a uniform target. The projectile has penetrated about half its diameter into the target, and intense shock waves (pressures in GPa) are radiating outward into the target from the interface. The projectile itself has become intensely compressed, and similar shock waves from the interface are spreading toward the rear of the projectile. When this shock wave reaches the rear of the projectile, it will be reflected forward as a tensional wave or **rarefaction,** unloading the projectile and allowing it to transform, virtually instantaneously, into melt and vapor. The original model, developed for large lunar impact events (*O'Keefe and Ahrens,* 1975), represents conditions about 1 s after the impact of a 46-km-diameter anorthosite projectile at 15 km/s onto a gabbroic anorthosite target, but similar conditions will be produced by smaller impacts and other material compositions. (Modified from *Melosh,* 1989, Fig. 4.1a, p. 47.)

The shock waves transmitted into the target rocks lose energy rapidly as they travel away from the impact point. Two factors are involved in this energy loss: (1) the expanding shock front covers an increasingly larger hemispherical area with increasing radial distance, thus reducing the overall energy density; (2) additional energy is lost to the target rocks through heating, deformation, and acceleration. The peak pressures of the shock waves therefore also drop rapidly with distance from the impact point. Theoretical models (*Melosh,* 1989, pp. 60–66) and geological studies of shock-metamorphosed rocks in individual structures (*Dence,* 1968; *Robertson,* 1975; *Grieve and Robertson,* 1976; *Dence et al.,* 1977; *Robertson and Grieve,* 1977; *Dressler et al.,* 1998) indicate that the peak shock-wave pressure ($\mathbf{P_s}$) drops exponentially with the distance **R** from the impact point according to an equation of the form $\mathbf{P_s} \boldsymbol{\alpha} \mathbf{R^{-n}}$. Various field and laboratory studies indicate a dependence of R^{-2} to $R^{-4.5}$; the exact value of the exponent depends on projectile size and impact velocity (*Ahrens and O'Keefe,* 1977).

On the basis of these studies, it is possible to regard the impact point as surrounded by a series of concentric, roughly hemispherical **shock zones,** each zone distinguished by a certain range of peak shock pressure (Fig. 3.2) and characterized by a unique suite of shock-metamorphic effects produced in the rocks. At the impact point, peak shock-wave pressures may exceed 100 GPa (= 1000 kbar or 1 Mbar) for typical cosmic encounter velocities, producing total melting, if not vaporization, of the projectile and a large volume of surrounding target rock. Further outward, pressures of 10–50 GPa may exist over distances of many kilometers from the impact point, producing distinctive shock-deformation effects in large volumes of unmelted target rock.

At even greater distances from the impact point, the peak shock-wave pressures eventually drop to about 1–2 GPa (*Kieffer and Simonds,* 1980). At this point, near the eventual crater rim, the shock waves become regular **elastic waves** or **seismic waves**, and their velocity drops to that of the velocity of sound in the target rocks (typically 5–8 km/s). These seismic waves can be transmitted throughout the entire Earth, like similar waves generated by earthquakes and volcanic eruptions. Because of their low pressures, they do not produce any permanent deformation of the rocks through which they pass. However, seismic waves may produce fracturing, brecciation, faulting, and (near the surface) landslides, and the results may be difficult to distinguish from those of normal geological processes.

The duration of the contact/compression stage is determined by the behavior of the shock wave that was reflected back into the projectile from the projectile/target interface (Fig. 3.1) (*Melosh,* 1989, pp. 57–59). When this shock wave reaches the back end of the projectile, it is reflected forward into the projectile as a **rarefaction** or **tensional wave** (also

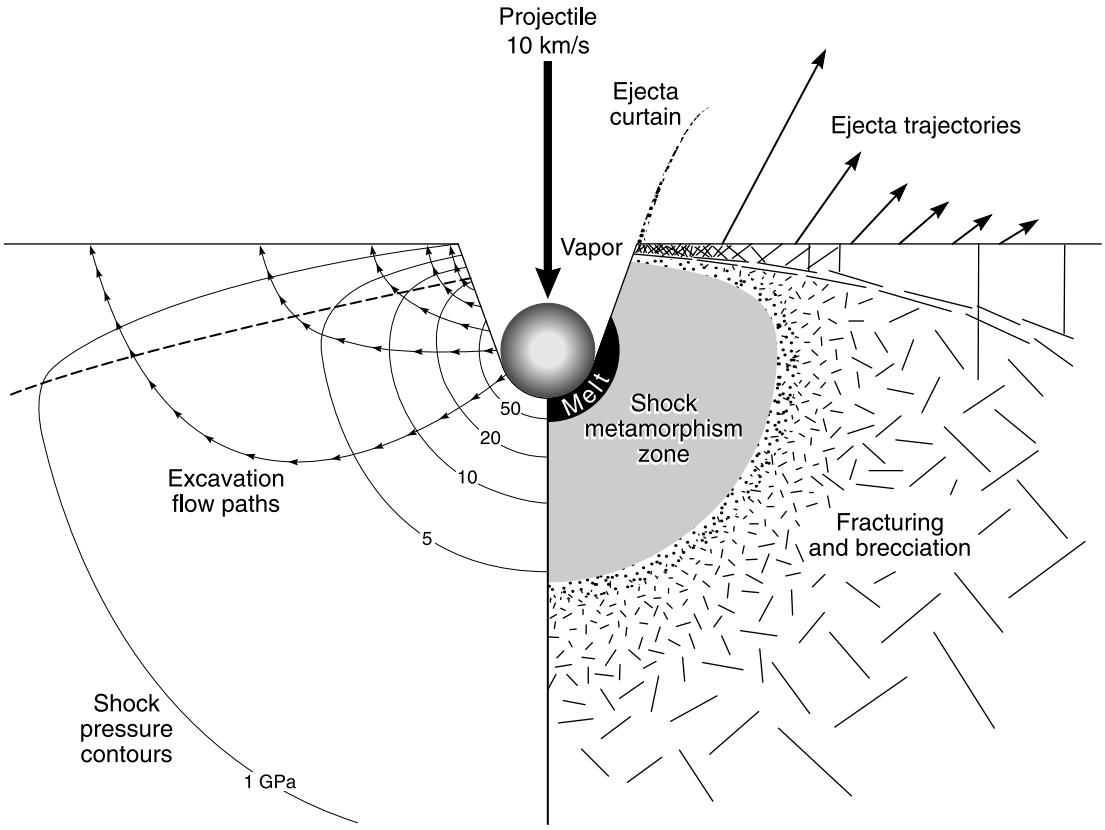

Fig. 3.2. Contact/compression stage: initial shock-wave pressures and excavation flow lines around impact point. Schematic cross-section showing peak shock pressure isobars (pressures in GPa) developed in the target around the impact point near the end of the contact/compression stage. The originally spherical projectile, after penetrating about two diameters into the target, has been almost completely destroyed and converted to melt and vapor. Shock waves radiating from the projectile-target interface decline rapidly outward in peak pressure (isobars in GPa on left side of cavity), creating concentric, approximately hemispherical zones of distinctive shock effects (right side of cavity). From the original interface outward, these zones involve: (1) melting (>50 GPa) and formation of a large melt unit; (2) shock-deformation effects (5–50 GPa); (3) fracturing and brecciation (1–5 GPa). The subsequent **excavation stage** involves two processes: (1) upward ejection (**spalling**) of large near-surface fragments and smaller ejecta (**ejecta curtain**) (upward-pointing arrows above ground surface); (2) subsurface flow of target material to form the **transient crater** (arrow paths crossing isobars at left side). (Modified from *Melosh,* 1989, Fig. 5.4, p. 64.)

called a **release wave**). As the release wave passes through the projectile from back to front, it **unloads** the projectile from the high shock pressures it had experienced. Because the shock pressures, and the associated temperatures, have been so high, this release results in the virtually complete melting and vaporization of the projectile. At the instant at which the release wave reaches the front end of the projectile, the whole projectile is unloaded, and the release wave continues forward into the target and begins to decompress it as well. This point, at which the release wave reaches the front of the projectile and begins to enter the adjacent compressed target, is taken as the end of the complete contact/compression stage.

The contact/compression stage lasts no more than a few seconds, even for impacts of very large objects. The time required for the shock wave to travel from the projectile/target interface to the rear edge of the projectile is approximately equal to the time it takes the projectile to travel the distance of one diameter at its original velocity. Even for large projectiles, this time is short: 2 s for a 50-km-diameter projectile traveling at 25 km/s, and less than 0.01 s for a 100-m-diameter object traveling at the same speed. The additional time required for the release wave to travel from the rear to the front edge will be no more than a few times this value, depending on the properties of projectile and target rock (*Melosh,* 1989, pp. 48 and 58). For most impact events, the entire contact/compression stage is over in less than a second.

After the release wave has reached the front end of the projectile and unloaded it completely, the projectile itself plays no further role in the formation of the impact crater, and the actual excavation of the crater is carried out by the shock waves expanding through the target rocks. The vaporized portion of the projectile may expand out of the crater as part

of a **vapor plume** (*Melosh,* 1989, pp. 68–71), and the remainder, virtually all melted, may be violently mixed into the melted and brecciated target rocks.

3.1.2. Excavation Stage: The Transient Crater

The brief contact/compression stage grades immediately into a longer **excavation stage,** during which the actual impact crater is opened up by complex interactions between the expanding shock waves and the original ground surface (Fig. 3.3) (*Melosh,* 1989, Chapter 5; *Grieve,* 1991). As the contact/compression stage ends, the projectile is surrounded by a roughly hemispherical envelope of shock waves that expand rapidly through the target rock. Because the projectile has penetrated a finite distance into the target, the center of this hemisphere actually lies within the original target rock at a point below the original ground surface.

Within this hemispherical envelope, the shock waves that travel upward and intersect the original ground surface are reflected downward as rarefactions (release waves). In a near-surface region where the stresses in the tensional release wave exceed the mechanical strength of the target rocks, the release wave is accompanied by fracturing and shattering of the target rock (Fig. 3.2). This reflection process also converts some of the initial shock-wave energy to kinetic energy, and the rock involved is accelerated outward, much of it as individual fragments traveling at high velocities (Fig. 3.4).

These complex processes drive the target rock outward from the impact point, producing a symmetric **excavation flow** around the center of the developing structure. Exact flow directions vary with location within the target rocks (Fig. 3.4). In the upper levels, target material moves dominantly upward and outward. At lower levels, target material moves dominantly downward and outward. These movements quickly produce a bowl-shaped depression (the **transient cavity** or **transient crater**) in the target rocks (*Maxwell,* 1977; *Grieve at al.,* 1977; *Grieve and Cintala,* 1981; *Melosh,* 1989, pp. 74–78).

The transient crater is divided into approximately equal upper and lower zones (Figs. 3.4 and 3.5). Within the upper **ejection zone,** velocities imparted to the target rocks may be as high as several kilometers per second, high enough to excavate the fragmented material and to eject it beyond the rim of the final crater (*Grieve et al.,* 1977; *Dence et al.,* 1977; *Kieffer and Simonds,* 1980; *Melosh,* 1989, pp. 74–76). Even at significant distances from the impact point, shock pressures and the resulting ejection velocities remain high enough (>100 m/s) to eject material. For this reason, the diameter of the final crater is many times larger (typically 20–30×) than the diameter of the projectile itself.

At deeper levels, tensional stresses in the release waves are lower. As a result, fracturing is less pronounced, excavation flow velocities are lower, and the excavation flow lines themselves are not oriented to eject material beyond the crater rim (Fig. 3.4). This region forms a **displaced zone** in which material is driven downward and outward more or less coherently.

Both zones in the transient crater continue to expand, accompanied by the uplift of near-surface rocks to form the **transient crater rim**, as long as the expanding shock waves and release waves are strong enough to eject or displace material from the developing cavity. However, these waves continually lose energy by deforming and ejecting the target rocks through which they pass. Eventually, a point is reached at which the shock and release waves can no longer excavate or displace target rock. At that point the growth of the transient crater ceases. There is an instant of theoretical balance in which the energies of the shock wave no longer act, and the waiting forces of gravity and rock mechanics have not yet reasserted themselves. At this instant, the transient crater reaches its maximum extent, the excavation stage ends, and the subsequent modification stage begins immediately.

The excavation stage, although longer than the contact/compression stage, is still brief by geological standards. If the near-surface excavation flow has a minimum average velocity of 1 km/s, then a 200-km-diameter transient crater can be excavated in less than 2 min. More detailed calculations (*Melosh,* 1989, p. 123) indicate that excavation of a l-km-diameter crater (e.g., Barringer Meteor Crater [Arizona]) will occur in about 6 s, while a 200-km-diameter crater requires only about 90 s.

The concept of the transient crater has been developed from a combination of theoretical studies (*Melosh,* 1989, Chapter 5) and geological investigations (*Dence,* 1968; *Grieve and Cintala,* 1981; *Grieve et al.,* 1981). The ideal transient crater is a bowl-shaped depression with a structurally uplifted rim (Figs. 3.4 and 3.5). Its shape is approximately hemispherical but is actually a paraboloid of revolution

Fig. 3.3. Development of a simple impact structure. Series of cross-section diagrams showing progressive development of a small, bowl-shaped simple impact structure in a horizontally layered target: **(a)** contact/compression stage: initial penetration of projectile, outward radiation of shock waves; **(b)** start of excavation stage: continued expansion of shock wave into target; development of tensional wave (**rarefaction** or **release wave**) behind shock wave as the near-surface part of original shock wave is reflected downward from ground surface; interaction of rarefaction wave with ground surface to accelerate near-surface material upward and outward; **(c)** middle of excavation stage: continued expansion of shock wave and rarefaction wave; development of melt lining in expanding transient cavity; well-developed outward ejecta flow (**ejecta curtain**) from the opening crater; **(d)** end of excavation stage: transient cavity reaches maximum extent to form melt-lined **transient crater;** near-surface ejecta curtain reaches maximum extent, and uplifted crater rim develops; **(e)** start of modification stage: oversteepened walls of transient crater collapse back into cavity, accompanied by near-crater ejecta, to form deposit of mixed breccia (**breccia lens**) within crater; **(f)** final simple crater: a bowl-shaped depression, partially filled with complex breccias and bodies of impact melt. Times involved are a few seconds to form the transient crater **(a)–(d)**, and minutes to hours for the final crater **(e)–(f)**. Subsequent changes reflect the normal geological processes of erosion and infilling.

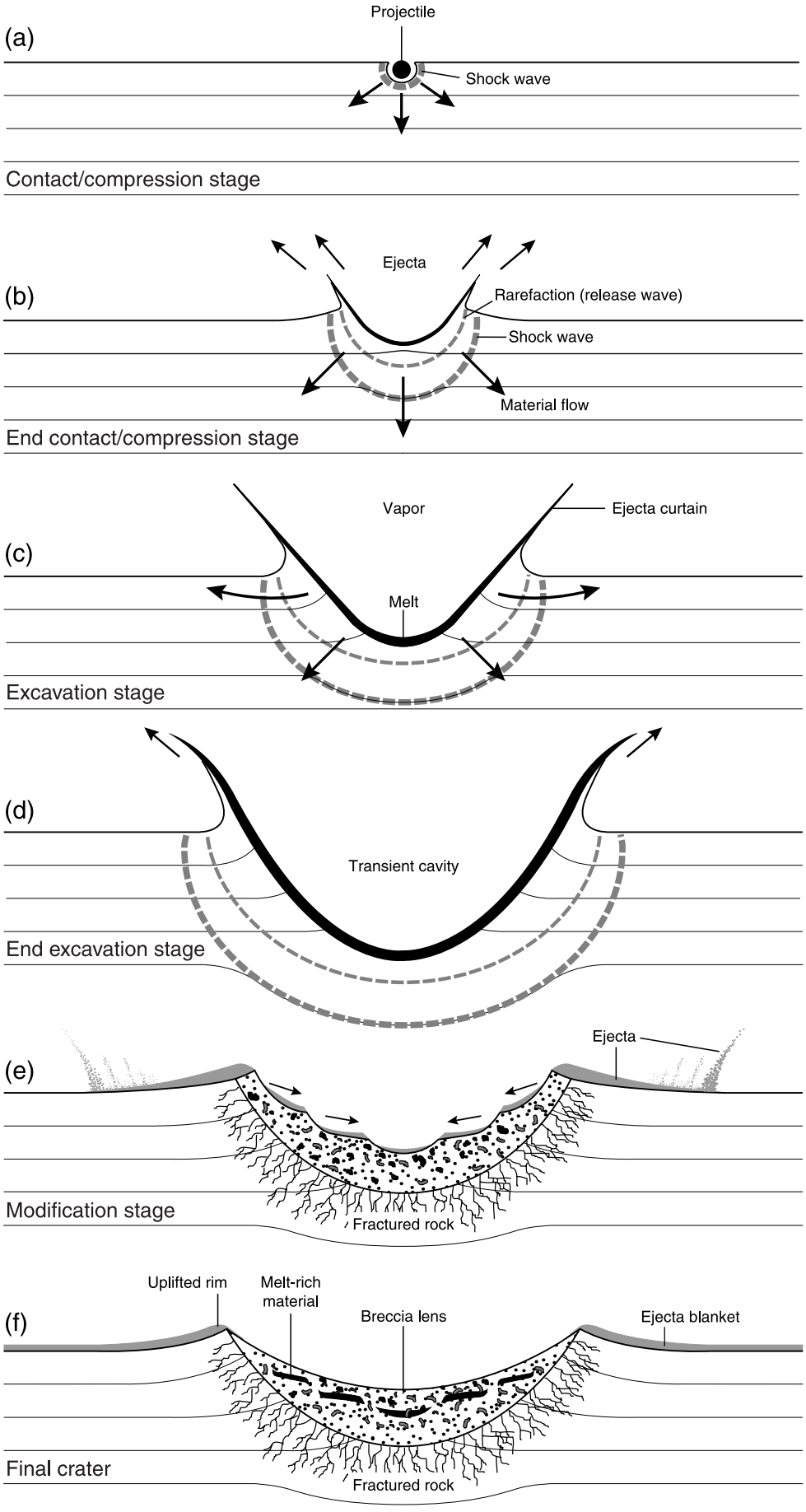
(a)
Projectile
Shock wave
Contact/compression stage
(b)
Ejecta
Rarefaction (release wave)
Shock wave
Material flow
End contact/compression stage
(c)
Vapor
Ejecta curtain
Melt
Excavation stage
(d)
Transient cavity
End excavation stage
(e)
Ejecta
Modification stage
Fractured rock
(f)
Uplifted rim
Melt-rich material
Breccia lens
Ejecta blanket
Final crater
Fractured rock

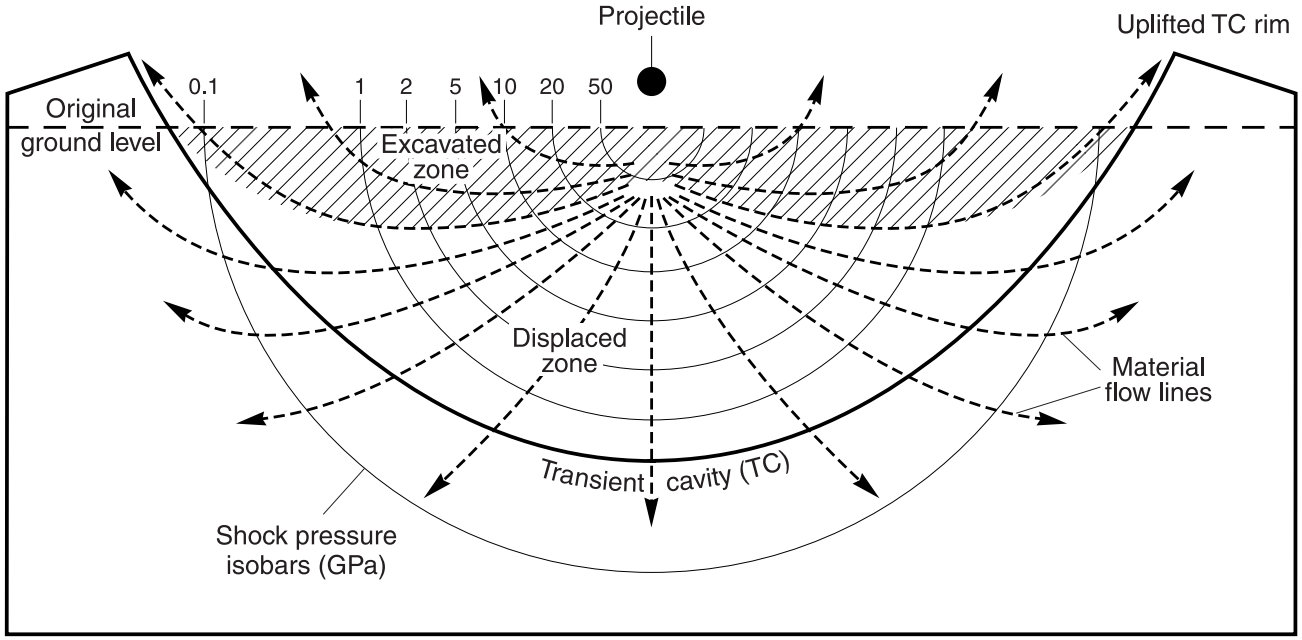

Fig. 3.4. Excavation stage: formation of transient crater. Theoretical cross section showing development of the transient crater immediately after the contact/compression stage. Original peak shock pressures (units in GPa) around the impact point are shown for simplicity as hemispherical isobars (for details, see Fig. 3.2). Complex interactions of the shock wave, the ground surface, and the subsequent rarefaction wave produce an outward **excavation flow** (dashed arrows) that opens up the transient crater. In the upper part of this region (**excavated zone**; ruled area), target material is fractured, excavated, and ejected beyond the transient crater rim. In the lower region (**displaced zone**), target material is driven downward and outward, more or less coherently, and does not reach the surface. This model yields two important geological results: (1) ejected material is derived only from the upper part (approximately the top one-third to one-half) of the transient cavity; (2) because the excavation flow lines in the excavated zone cut across the initially hemispherical shock isobars, ejected material will reflect a wide range of original shock pressures and deformation effects, ranging from simple fracturing to complete melting and vaporization. (Modified from *Grieve,* 1987, Fig. 5; *Hörz et al.,* 1991, Fig. 4.3a, p. 67.)

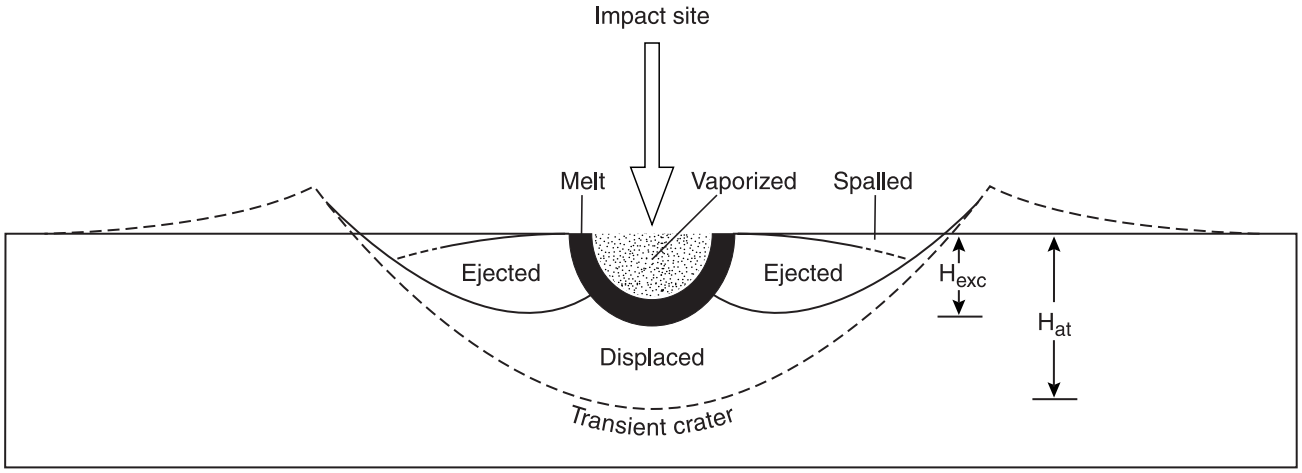

Fig. 3.5. Transient crater: locations of shock-metamorphosed materials. Cross section through a theoretical transient crater, showing discrete zones from which various shock-metamorphosed materials are derived. The "vaporized" zone closest to the original impact point (stippled) contains a mixture of vaporized target rock and projectile, which expands upward and outward into the atmosphere as a **vapor plume**. The adjacent "melt" zone (solid black) consists of melt that moves downward and then outward along the floor of the final transient cavity (for details, see Fig. 6.2). Material in the upper "ejected" zones on either side of the melt zone, which contains a range of shock-metamorphic effects, is ejected outward to and beyond the transient crater rim. The lower "displaced" zone moves downward and outward to form the zone of **parautochthonous** rocks below the floor of the final transient crater. $\mathbf{H_{at}}$ = the final transient crater depth; $\mathbf{H_{exc}}$ = the depth of excavation, which is significantly less than the total depth. (From *Melosh,* 1989, Fig. 5.13, p. 78.)

(*Dence,* 1973). Its maximum depth is approximately one-third its diameter, and this proportion seems to remain approximately constant for craters of widely different size (*Maxwell,* 1977; *Croft,* 1985).

The theoretical instant of ideal overall balance in a transient crater at the end of the excavation stage may not be actually attained during formation of a real crater. For example, in these models, the maximum diameter is normally attained after the maximum depth is reached. Subsequent modification of one part of an actual transient crater might therefore begin while other parts are still being excavated. Even so, the transient crater is a key concept in models of crater formation. All impact structures, regardless of their final size or the complexity of their subsequent development, are assumed to pass through the transient-crater stage, making this stage of critical importance in comparing impact structures of different sizes or on different planets. Defining the transient crater is also an essential step in determining critical characteristics of an impact structure: its original (pre-erosion) diameter and depth, the energy of impact, the size and velocity of the projectile, the distribution of shock pressures and shock effects within the crater, the amount of material melted and ejected during formation of the crater, the amount of structural uplift during formation of the central peak of complex impact structures, and the depth from which excavated materials were derived.

3.1.3. Modification Stage

The excavation stage ends when the transient crater has grown to its maximum size, and the subsequent modification stage begins immediately. The expanding shock waves have now decayed to low-pressure elastic stress waves beyond the crater rim, and they play no further part in the crater development. Instead, the transient crater is immediately modified by more conventional factors like gravity and rock mechanics.

The immediate part of the modification stage, during which the major impact-related changes occur, lasts only slightly longer than the excavation stage: less than a minute for a small structure, a few minutes for a large one (*Melosh,* 1989, Chapter 8, pp. 141–142). (One simple definition is that the modification stage ends "when things stop falling.") However, the modification stage has no clearly marked end, and the modification processes of uplift and collapse merge gradually into the normal processes of geological mass movement, isostatic uplift, erosion, and sedimentation.

3.2. SIMPLE AND COMPLEX IMPACT STRUCTURES

The extent to which the transient crater is altered during the modification stage depends on its size and (to a lesser extent) on the structure and properties of the target rock. Small transient craters are altered chiefly by the collapse of their upper walls, and the shape of the final crater is little changed from that of the original transient crater. In larger structures, modification may involve major structural changes: uplift of the central part of the floor and major peripheral collapse around the rim. Depending on the extent to which the transient crater is modified, three distinct types of impact structures can be formed: **simple craters**, **complex craters**, and **multiring basins.**

3.2.1. Simple Craters

The smallest impact structures occur as bowl-shaped depressions (**simple craters**) less than a few kilometers across, which help to preserve the shape and dimensions of the original transient cavity (Figs. 1.1 and 3.6). In evolving to a simple crater, the transient crater is modified only by minor collapse of the steep upper walls into the crater cavity and by redeposition of a minor amount of ejected material in the crater. As a result, the crater diameter may increase by as much as 20%, but the original transient crater depth remains largely unaffected (Fig. 3.7) (*Melosh,* 1989, p. 129).

During modification, the simple crater is immediately filled, to perhaps half its original depth, by a mixture of redeposited (**fallback**) ejecta and debris slumped in from the walls and rim (Fig. 3.7). This crater-filling unit, variously called the **breccia lens** or **crater-fill breccia**, is a mixture of rock fragments, both shocked and unshocked, together with fragments or lenses of shock-melted rock (**impact melt**).

Fig. 3.6. A simple lunar impact crater. This small, well-preserved crater (Moltke: D = 7 km) shows features typical of simple impact craters: a circular outline, a bowl-like shape, an uplifted rim, and hummocky deposits of ejecta around the rim. In the relatively low gravity of the Moon, this structure formed as a simple crater; a terrestrial structure of the same diameter, formed under Earth's higher gravity, would have formed as a complex crater with a central uplift. (Apollo 10 image AS10-29-4324.)

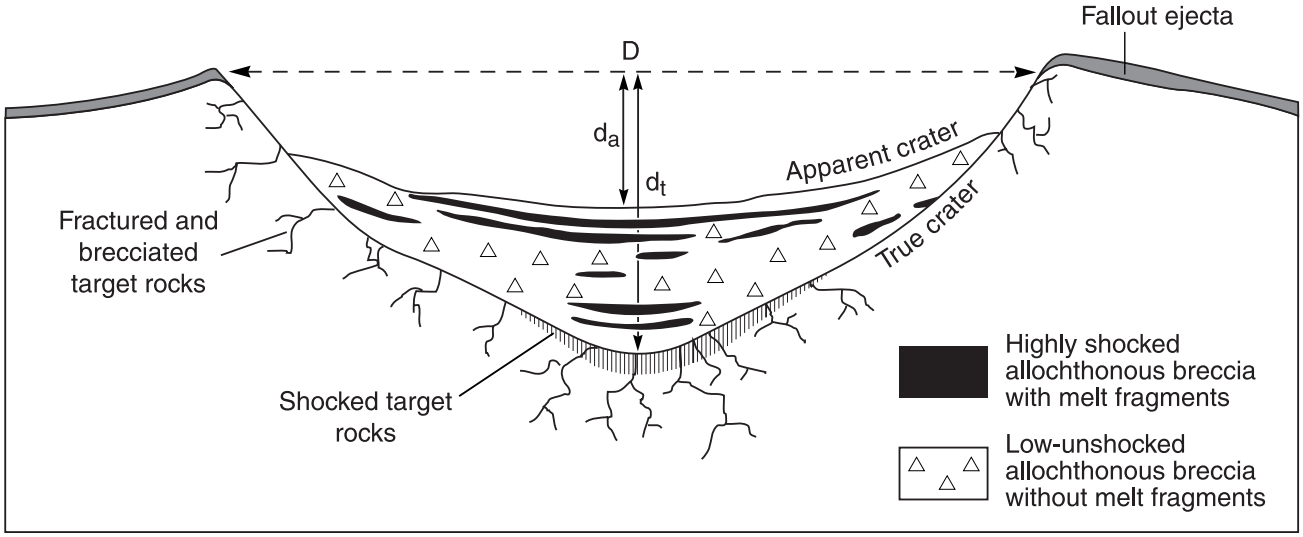

Fig. 3.7. Simple impact structure: locations of impactite types. Schematic cross section of a typical simple impact structure, showing the simple bowl shape and the locations of various types of impactites in and around the structure. The **parautochthonous** rocks below the true crater floor are fractured and brecciated but generally show no distinctive shock effects, except in a small zone (fine vertical ruling) in the center of the structure. The crater is filled, to approximately half its original height, with a variety of **allogenic** breccias and impact melts, which forms the **crater-fill units** or the **breccia lens**. A thinner layer of ejected material (**fallout ejecta**) overlies the uplifted crater rim and surrounds the crater. This unit is easily eroded and is present only in the youngest and best-preserved structures. **D** = final crater diameter, which is 10–20% greater than the diameter of the original, premodification transient crater; $\mathbf{d_t}$ = **true depth** of the final crater, which is approximately the depth of the original transient crater; $\mathbf{d_a}$ = **apparent depth** of the crater, or the depth from the final rim to the top of the crater-fill units. The diagram represents the state of the final crater before any subsequent geological effects, e.g., erosion, infilling. The model is based on drilling studies at Barringer Meteor Crater (Arizona) (*Roddy et al.,* 1975; *Roddy,* 1978), Brent Crater (Canada) (*Dence,* 1968; *Grieve and Cintala,* 1981), and similar structures (e.g., *Masaitis et al.,* 1980; *Gurov and Gurova,* 1991). (From *Grieve,* 1987, Fig. 1.)

Depending on the subsequent geological history, the breccia lens may be eroded or may be covered and preserved by a cap of later sedimentary fill.

3.2.2. Complex Craters

The bowl-shaped form of simple craters appears only in relatively small structures less than a few kilometers across. Larger impact structures (**complex craters**) display a different and more complicated form, characterized by a centrally uplifted region, a generally flat floor, and extensive inward collapse around the rim (Figs. 1.3, 3.8, and 3.9) (*Dence,* 1968; *Grieve et al.,* 1977, 1981; *Grieve,* 1991). For terrestrial structures, the transition between simple and complex craters occurs at a diameter of about 4 km in massive crystalline rocks, but at only about 2 km in sediments. (However, these values apply only to Earth. The transition diameter varies inversely with gravitational acceleration, and it is different on different planets.) The larger impact events that form complex craters apparently release enough energy to overcome the fundamental strength of the target rocks over a large volume beneath the large transient crater. As a result, late-stage modification involves complex interactions between shock-wave effects, gravity, and the strength and structure of the target rocks, and the modification is characterized by outward, inward, and upward movements of large volumes of the subcrater rocks.

The details of these interactions are uncertain, but the general result is that the original bowl-shaped transient crater is immediately modified as deep-seated rocks beneath the center of the transient crater rise to form a **central uplift** (*Dence,* 1968; *Grieve et al.,* 1981). At the same time, rocks around the periphery of the transient crater collapse downward and inward along concentric faults to form one or more depressed rings (**ring grabens**) and a series of terraces along the outer margins of the final structure (Fig. 3.10). [A simple model of the formation of a complex crater and its central uplift is presented by the familiar slow-motion movies of a drop of liquid hitting a liquid surface (e.g., *Melosh,* 1989, p. 148; *Taylor,* 1992, p. 168). There is the same initial cavity formation, the same outward and downward ejection of target material, the same upward rebound of the central cavity floor, and the same collapse of the periphery back into the cavity. However, in impact events, these processes take place in solid rock and may operate over distances of tens to hundreds of kilometers.]

The idea that such rapid deformation and subsequent uplift can occur in large volumes of crustal rocks has been difficult for many geologists to appreciate. Key evidence has come from studies of impact structures formed in sedimentary rocks, in which the actual uplift of key stratigraphic markers has been established beyond question through drilling and geophysical studies (e.g., *Milton et al.,* 1972, 1996a,b;

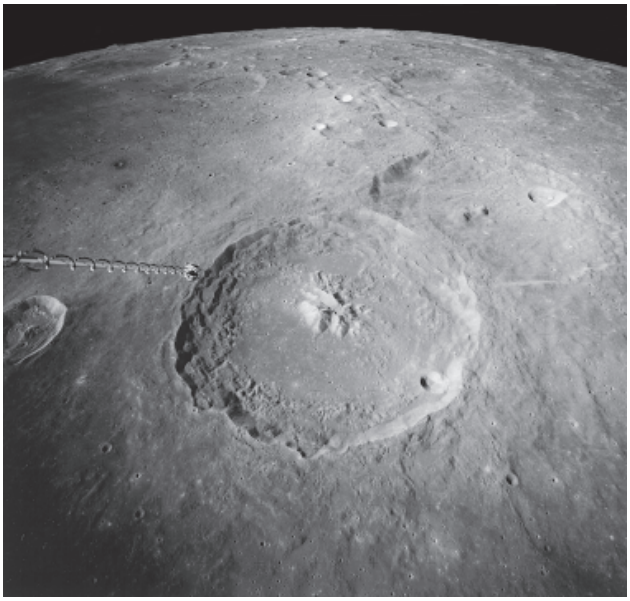

Fig. 3.8. A complex lunar crater. This relatively young crater (Theophilus: D = 100 km) displays well-preserved features that are typical of complex impact structures: a central uplift, a scalloped circular outline, ruggedly terraced walls with possible landslide deposits inside the rim, and hummocky ejecta deposits just outside the rim. This view also indicates the continuing nature of lunar cratering; an older impact crater (upper right) has been partly destroyed by Theophilus, while a younger small crater has formed within Theophilus itself (near rim, lower right). The flat dark area in the background (upper left) is made up of lava flows covering part of Mare Nectaris. The spiral-like rod at left center is an instrument boom on the Apollo 16 spacecraft, from which this orbital picture was taken. (Apollo 16 image AS16-M-0692.)

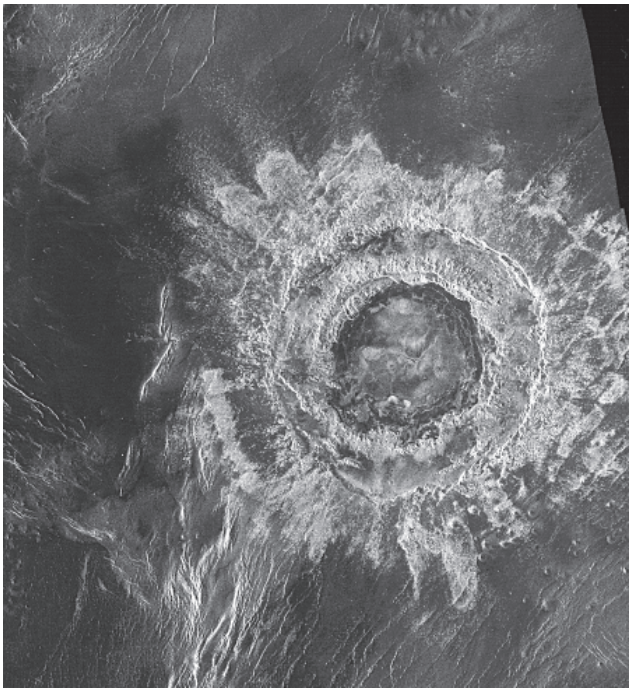

Fig. 3.9. A complex impact basin on Venus. A large, well-preserved multiring impact basin on the surface of Venus (Meitner: D = 150 km) is revealed beneath the planet's opaque atmosphere by the imaging radar system of the Magellan spacecraft. Meitner, the third-largest impact structure identified on Venus, shows a flat smooth (dark-colored) interior, two circular rings, and a rough, irregular blanket of lobate ejecta (light-colored). The crater was formed on a surface of smooth plains, possibly underlain by lava flows and cut by abundant parallel fractures (white lines). (Magellan image F-MIDRP .55S319;201.)

Grieve et al., 1981; *Grieve and Pilkington,* 1996). Geological studies have also established that the amount of actual **stratigraphic uplift** (**SU**) in impact structures is about one-tenth the final diameter (**D**) of the structure. A detailed statistical relation derived from studies of well-constrained complex impact structures (*Grieve et al.,* 1981, p. 44) is $\mathbf{SU = 0.06\ D^{1.1}}$ (both SU and D are in kilometers). A subsequent analysis, using more craters (*Grieve and Pilkington,* 1996, p. 404), gave $\mathbf{SU = 0.086\ D^{1.03}}$. The two equations are virtually identical, and a value of SU = 0.1 D is a reasonable approximation to either. For large (D = 100–200 km) impact structures, these relations imply that the crustal rocks beneath the structure are uplifted vertically by 10–20 km during the impact event. An uplift of this magnitude has been estimated for the Vredefort (South Africa) structure on geological grounds (*Reimold and Gibson,* 1996; *Therriault et al.,* 1997; *Turtle and Pierazzo,* 1998).

Both theoretical and field studies indicate that central uplifts form in only a few minutes, almost instantaneously by geological standards, even in the largest structures (*Melosh,* 1989, pp. 129 and 141–142). Theoretical studies also suggest that the central uplifts of structures 200–300 km in diameter, such as Vredefort (South Africa), formed in less than 15 minutes (*Melosh,* 1989, pp. 141–142; *Turtle and Pierazzo,* 1998).

Despite the extensive evidence that central uplifts do form in large impact structures, the details of the process are still the subject of continuing uncertainty and active debate (*Dence,* 1968; *Grieve et al.,* 1981; *Melosh,* 1989, Chapter 8; *Hörz et al.,* 1991; *Spudis,* 1993). Even so fundamental a quantity as the ratio between the diameter of the initial transient crater and the diameter of the final complex impact structure has not been well established; values estimated by various workers, using both theoretical and geological studies, range from about 0.5 to 0.7 (see, e.g., *Therriault et al.,* 1997, Table 2).

At larger crater diameters, the resulting structures, and especially the centrally uplifted area, become even more complicated. As the crater size increases the character of the central uplift changes, and the single central peak is progressively replaced by a more complex series of concentric rings and basins. At least three types of complex impact structures can be distinguished with increasing crater diameter: **central-peak structures**, **central-peak-basin structures**, and **peak-**

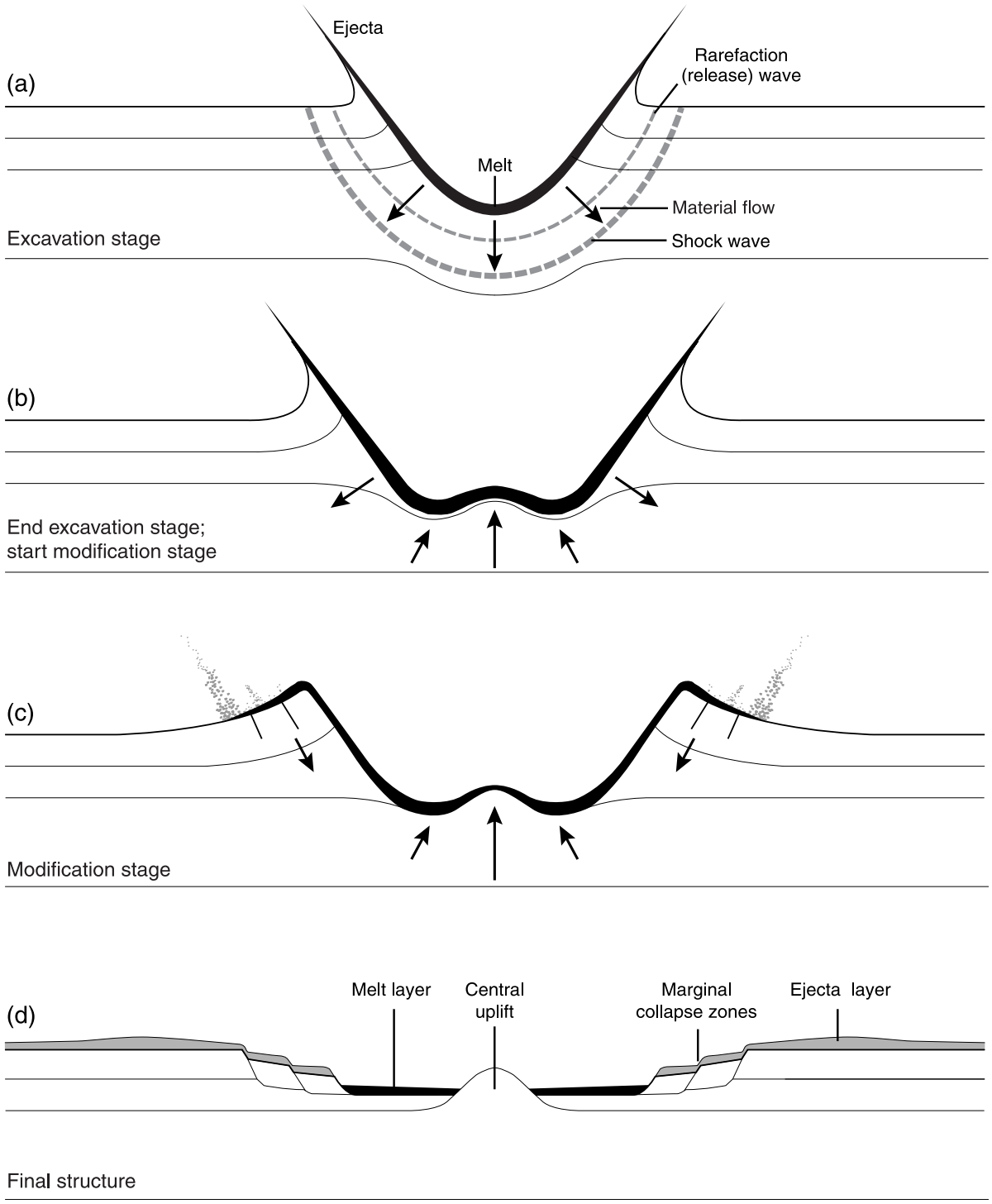

Fig. 3.10. Development of a complex impact structure. Series of cross sections showing progressive development of a large, complex impact structure in a horizontally layered target: **(a)** formation of a large transient crater by the excavation process is virtually identical to transient crater formation in smaller structures (compare with Fig. 3.3a–d); **(b)** initial development of central uplift during the subsequent modification stage; **(c)** start of peripheral collapse, accompanied by continuing development of the central uplift and the thinning and draping of the original melt layer (black) over the uplifted rocks; **(d)** final structure, which is of the central-uplift type, consists of a central uplift of deeper rocks, surrounded by a relatively flat plain and by a terraced rim produced by inward movement along stepped normal faults. The central uplift is surrounded by an annular deposit of **allogenic** breccias and impact melt (black), which may be absent from the central peak itself. An ejecta layer (stippled) covers the target rocks around the structure. The diameter of the final structure, measured at the outer rim beyond the outermost fault, may be 1.5–2× the diameter of the original transient crater. This central-peak morphology is observed in terrestrial structures ranging from about 2–25 km in diameter; larger structures tend to develop one or more concentric rings within the crater (for details, see text).

ring basin structures (*Grieve at al.,* 1981; *Melosh,* 1989, Chapter 8; *Spudis,* 1993). As the terms suggest, these structures are characterized by the initial development of a basin in the central peak and eventually by the complete conversion of the central peak area to a ring structure (Figs. 1.3, 3.9, and 3.11).

These distinctions, and the transition diameters at which they occur, have been most clearly established on airless bodies like the Moon, where even large ancient structures have been well preserved (Figs. 3.6, 3.8, and 3.11) (e.g., *Taylor,* 1982, 1992; *Melosh,* 1989, pp. 131–135; *Spudis,* 1993). Classification of large terrestrial structures (e.g., papers in *Schultz and Merrill,* 1981; *Spudis,* 1993, pp. 24–41) is more difficult and uncertain, because the impact structures, especially their critical upper parts, tend to be removed by erosion or buried by later sediments. Furthermore, the critical diameters at which one form changes to another depend inversely on the planetary gravity, making it difficult to apply data from structures on other planets to terrestrial features. For example, the transition between simple and complex craters occurs at about 20 km diameter on the Moon but at only 2–4 km on Earth. The subsequent transition between a central-peak-basin structure to a peak-ring structure occurs at about 150–200 km on the Moon, but at only about 20–25 km on Earth.

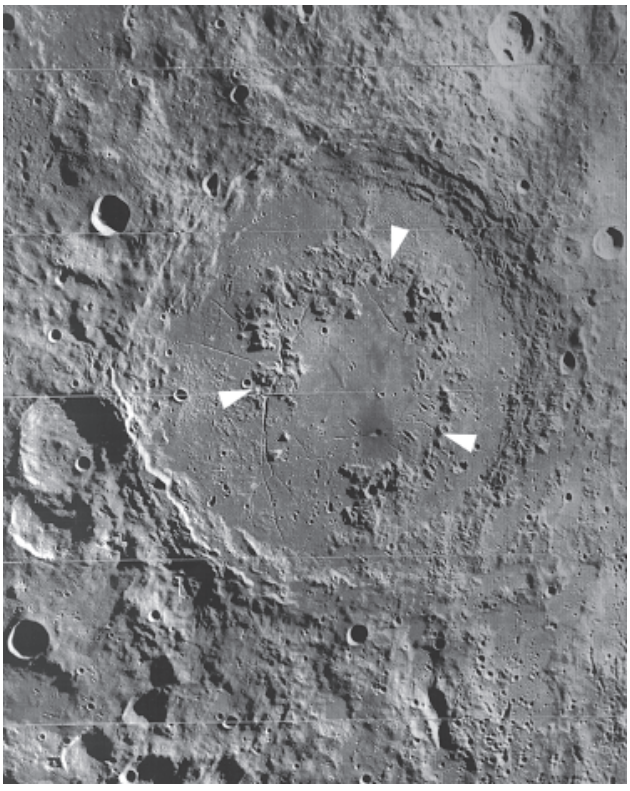

Fig. 3.11. A lunar impact basin. This large impact structure (Schrödinger: D = 320 km) is located on the lunar farside near the Moon's South Pole. Although ancient and highly degraded, it still preserves features distinctive of larger complex impact structures: a central uplift and terraced walls. However, in this large structure, the central uplift appears as an interior peak ring about 150 km in diameter (arrows), in sharp contrast to the simpler central peak formed in smaller complex structures. (Lunar Orbiter image LO-IV-8M.)

Despite the various difficulties, it has been possible to establish rough boundaries for different types of terrestrial complex structures (*Grieve et al.,* 1981, p. 42, Fig. 2). These limits, and some typical examples, are: central-peak structures (D = 4–22 km) [Steinheim (Germany), Sierra Madera (Texas)]; central-peak-basin structures (D = 22–30 km) [Mistastin (Canada)]; peak-ring-basin structures (D = 30–62 km) [West Clearwater (Canada); Fig. 1.3]. These values are only approximations, and they will almost certainly change as more structures are studied in detail and as the formation of complex craters is better understood.

3.2.3. Multiring Basins

The largest planetary impact structures so far identified have diameters of a few hundred kilometers to more than 1000 km (e.g., papers in *Schultz and Merrill,* 1981; *Melosh,* 1989, Chapter 9; *Spudis,* 1993). In contrast to smaller impact structures, they appear as huge geological bulls-eyes, composed of multiple concentric uplifted rings and intervening down-faulted valleys (**ring grabens**) (Fig. 3.12). These features, designated **multiring basins**, are defined as structures that have two or more interior rings in addition to the outer rim of the structure.

Multiring impact basins have been produced by the impact of projectiles tens to hundreds of kilometers in diameter, and they date mainly from an early period in the solar system (≥3.9 Ga), when such large objects were more abundant and collisions were more frequent. The best multiring basins are best observed on planets with well-preserved ancient surfaces, such as the Moon, Mercury, parts of Mars, and some of the moons of Jupiter. Mare Orientale, on the Moon, with a diameter of at least 900 km, is one of the most prominent and best-known multiring basins (Fig. 3.12), but even larger features exist, such as the Valhalla Basin (D ~4000 km) on Jupiter's icy moon Callisto. In addition, there are numerous large basins in the solar system that do not display a pronounced multiring structure, possibly because they have been deeply eroded since they formed. These include the Caloris Basin (Mercury; D = 1300 km), the Argyre Basin (Mars; D > 900 km) (Fig. 1.9), and the recently identified South Pole-Aitken Basin on the Moon (D ~2500 km).

On the Moon, the transition to multiring basins occurs at diameters of about 400–600 km. Because the transition diameters for different crater forms vary inversely with planetary gravity, this observation implies that multiring basins should begin to form on Earth at crater diameters greater than about 100 km. Because the few terrestrial impact structures in this size range have been deeply eroded or buried (e.g., Fig. 1.4), it has not yet been possible to demonstrate clearly that any multiring basins exist on the Earth. The few possible candidates (and their current estimated diameters) are Manicouagan (Canada, 100 km), Popigai (Russia, 100 km), Vredefort (South Africa, >200 km), Sudbury

Fig. 3.12. A lunar multiring impact basin. One of the largest, freshest, youngest, and best-known multiring impact basins in the solar system, Mare Orientale (D = 930 km) lies on the boundary between the Earth-facing lunar nearside (right) and the lunar farside. The structure, formed at about 3.8 Ga, is bounded by an outer ring about 930 km in diameter (Cordillera Mountains), and inner rings with diameters of 620, 480, and 320 km can be distinguished. Mare Orientale is surrounded by radial features (especially at lower right) that may have been produced by the low-angle ejection of large blocks of excavated material. The postimpact history of the structure is also complex, and much of the area inside the rings has been modified by later volcanic activity. The flat dark areas at upper right are the younger lava flows that cover Oceanus Procellarum. (Lunar Orbiter image LO-IV-187M.)

(Canada, >200 km), and Chicxulub (Mexico, >180 km). It has not proved possible to establish beyond question the multiring character of these structures for various reasons, including deep erosion, postcrater deformation, or insufficient geological study. The strongest current candidate for a terrestrial multiring structure is Chicxulub, which, although buried, appears well preserved (*Sharpton et al.,* 1993, 1996b; *Morgan et al.,* 1997).

Multiring basins represent the most energetic and catastrophic impact events in the solar system, and the postimpact movements — upward, downward, and inward — of the target rock that modify the transient crater are far more complex and widespread than in smaller structures. It is therefore not surprising that the formation of multiring basins is even more uncertain and hotly debated than is the origin of smaller complex impact structures (e.g., papers in *Schultz and Merrill,* 1981; *Melosh,* 1989, Chapter 9; *Spudis,* 1993).

For example, it is not clear whether the transition between smaller impact structures and multiring basins is a natural development with increasing crater diameter (*Herrick et al.,* 1997), or whether multiring basins only form when special conditions are present within the target, e.g., a crust-mantle structure with a weak layer (*asthenosphere*) at depth within the planet (see *Melosh,* 1989, pp. 176–180). Nor is it understood why some planetary features in the 1000–2000-km-diameter range have a pronounced multiring form (Fig. 3.12) and others do not (Fig. 1.9). Finally, it is not yet established whether multiring impact structures — ancient or modern — do exist on Earth and which large structures they may be.

3.3. SUBSEQUENT DEVELOPMENT OF IMPACT STRUCTURES

When the crater formation process ends, the resulting circular structure, whether simple or complex, consists of deformed subcrater rocks covered by an **ejecta blanket** outside the crater and with **crater-fill deposits** (usually a mixture of breccias and bodies of impact melt) within it (Figs. 3.7 and 3.13). This assemblage of distinctive near-surface rocks is immediately subject to more normal geological processes: erosion, burial, and tectonic deformation. If the crater forms on land and remains exposed after formation, erosion will quickly remove the surface ejecta blanket and destroy any surviving meteorite fragments. At the same time, however, a lake may form in the crater depression, covering the crater-fill material with a preserving cap of sediments, e.g., as at Brent (Canada) (*Dence,* 1968; *Grieve,* 1978) and the Ries Crater (Germany) (*von Engelhardt,* 1990).

If the original impact site is covered by water, the formation and subsequent history of the resulting crater may be more complex. At the moment of impact, the overlying layer of water will be excavated with the underlying bedrock, and the development of the crater and the deposition of the impact-produced rock units will be modified by the immediate and violent **resurge** of this displaced water back into the crater cavity (*Therriault and Lindström,* 1995; *Lindström et al.,* 1996). If the crater remains below the water level, it will immediately begin to fill with sediments, and its subsequent history will depend on whether it remains below water level (continuous sediment filling) or is uplifted at some future time (beginning of erosion). A number of such submarine impact structures have now been recognized; some have subsequently been raised above sea level [e.g., Lockne (Sweden) (*Therriault and Lindström,* 1995; *Lindström et al.,* 1996)] and others still remain buried [e.g., Montagnais (Canada) (*Jansa and Pe-Piper,* 1987); the Chesapeake Bay Crater (USA) (*Poag,* 1996, 1997); and the recently discovered Mjølnir structure (Norway) in the Barents Sea (*Dypvik et al.,* 1996)].

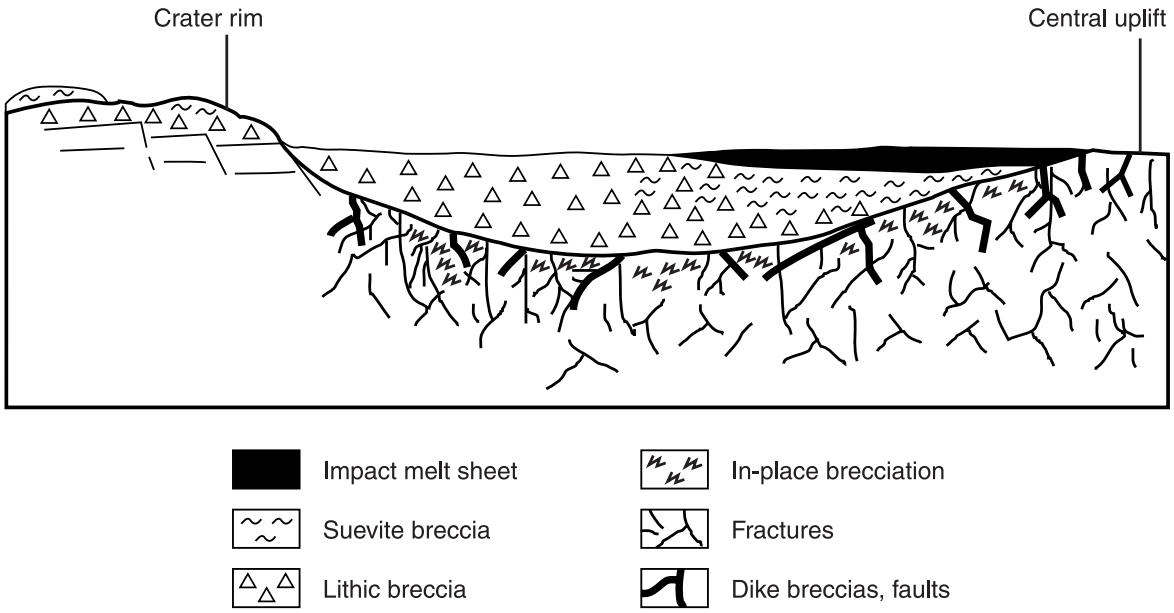

Fig. 3.13. Complex impact structure: locations of impactite types. Schematic radial cross section across a complex impact structure of the central-uplift type, from the central uplift (right) to the outer, downfaulted rim (left). (Vertical scale is exaggerated.) The subcrater **parautochthonous** rocks, exposed in the central uplift, are highly fractured and brecciated and may contain distinctive shock features such as shatter cones. These rocks may also contain widespread **pseudotachylite** breccias and dike-like intrusive bodies of **allogenic** breccias and impact melts. Larger and thicker subhorizontal units of allogenic breccias and melts occur as an annular unit of **crater-fill material** that covers the parautochthonous rocks between the central uplift and the rim. The bulk of these crater-fill deposits consist of melt-free **lithic breccias**, with lesser amounts of melt-bearing **suevite** breccias. The melt component in the crater-fill deposits becomes more abundant toward the center and upward, and a discrete layer of impact melt (solid black) may occur at or toward the top of the crater fill. (Modified from *Stöffler et al.,* 1988, Fig. 12, p. 290.)

Because impact is a near-surface process, the deformation associated with impact structures dies away rapidly with depth. Typical impact structures are relatively shallow, and impact-produced rocks form comparatively thin units. The distinctive rock types and shock effects in a structure tens of kilometers in diameter may extend only a few kilometers below the original ground surface. Impact structures are therefore especially vulnerable to erosion. Initial erosion will preferentially remove the near-surface ejecta deposits and the distinctively shocked and melted materials they contain, thus rapidly destroying the most convincing evidence for impact. Deeper erosion over longer periods of time will eventually produce major destructive changes in the crater. The breccias and melt units that fill the crater, and the distinctive shocked materials they contain, together with any protecting cap of sediments, will be reduced to small remnants or completely removed. The original circular outline will disappear. Eventually, all trace of the crater will be removed except for the weakly shocked subcrater rocks. If erosion continues long enough, the whole impact structure will be erased.

Impact structures that are not destroyed by erosion may be entirely filled and buried by younger sediments, so that their detection depends on geophysical methods and drilling rather than on surface field geology. About one-third of the presently known impact structures are subsurface (*Grieve,* 1991, 1997; *Grieve and Masaitis,* 1994; *Grieve et al.,* 1995); they were first discovered during geophysical explorations, and their impact origin has been verified by the discovery of shocked rocks in drill core samples. This group includes several continental structures that are actual or potential petroleum producers [Ames (Oklahoma); Avak (Alaska); Marquez (Texas); Red Wing Creek (North Dakota)] (*Donofrio,* 1997), as well as a few submarine impact structures [e.g., Montagnais (Canada) (*Jansa and Pe-Piper,* 1987)]. Several large and relatively young buried impact structures have also been identified by geophysical techniques: the 90-km-diameter Chesapeake Bay Crater (USA) (*Poag,* 1996, 1997); the larger (>180-km diameter) Chicxulub structure (Mexico), which is associated with the K/T event (*Hildebrand et al.,* 1991; *Sharpton et al.,* 1992; papers in *Ryder et al.,* 1996); and the large (≥70 km?) Morokweng structure (South Africa) (*Corner et al.,* 1997; *Koeberl et al.,* 1997a). Many more impact structures remain to be found, and the evidence for their existence may already be sitting unrecognized in existing drill cores and geophysical records around the world.

Impact structures may also be caught up in subsequent tectonic deformation, with varying results. Horizontal compression may deform the original circular shape, making study and interpretation more difficult [as at Sudbury (Canada)].

Tectonism can also break up regions of original shocked rocks and disperse them as large discrete areas across the geological landscape [e.g., the Beaverhead (Idaho) structure (*Hargraves et al.,* 1990; *Fiske et al.,* 1994)]. Sufficient tectonism and metamorphism could destroy even large impact structures or make them totally unrecognizable.

Geologists must therefore be prepared to recognize impact structures in all states of preservation, from young, fresh, well-exposed circular structures filled with distinctive shocked breccias to older features in which distinctive shock effects are scattered, barely recognizable, or deeply buried. It is essential to be able to recognize the variety of distinctive shock effects associated with impact structures and to understand where different types of shock effects may be located in the original crater.